Nuclear Engineering and Technology xxx (xxxx) xxx

Contents lists available at ScienceDirect

Nuclear Engineering and Technology

journal homepage: www.elsevier.com/locate/net

Original Article

Simulation on mass transfer at immiscible liquid interface entrained by single bubble using particle method

Chunhui Dong, Kailun Guo, Qinghang Cai, Ronghua Chen*, Wenxi Tian, Suizheng Qiu, G.H. Su**

School of Nuclear Science and Technology, Shaanxi Engineering Research Center of Advanced Nuclear Energy, State Key Laboratory of Multiphase Flow in Power Engineering, Xi'an Jiaotong University, Xi'an, 710049, China

ARTICLE INFO

Article history:
Received 13 March 2019
Received in revised form
27 August 2019
Accepted 20 November 2019
Available online xxx

Keywords:
Moving particle semi-implicit (MPS) method
MCCI
Mass transfer
Immiscible liquids interface

ABSTRACT

As a Lagrangian particle method, Moving Particle Semi-implicit (MPS) method has great capability to capture interface/surface. In recent years, the multiphase flow simulation using MPS method has become one of the important directions of its developments. In this study, some key methods for multiphase flow have been introduced. The interface tension model in multiphase flow is modified to maintain the smooth of the interface and suitable for the three-phase flow. The mass transfer at immiscible liquid interface entrained by single bubble which could occur in Molten Core-Concrete Interaction (MCCI) has been investigated using this particle method. With the increase of bubble size, the height of entrainment column also increases, but the time of film rupture is slightly different. With the increase of density ratio between the two liquids, the height of entrained column decreases significantly due to the decreasing buoyancy of the denser liquid in the lighter liquid. In addition, the larger the interface tension coefficient is, the more rapidly the entrained denser liquid falls. This study validates that the MPS method has shown great performance for multiphase flow simulation. Besides, the influence of physical parameters on the mass transfer at immiscible interface has also been investigated in this study.

1. Introduction

The immiscible stratified liquids are inevitable in the fields of metallurgical industry and nuclear reactor safety. In the former, the lighter slags float on the heavier molten metal. Meantime, the manual injection of gas agitates the immiscible interface between the two phases. This process is called emulsion, which could improve the interaction efficiency, reduce the energy consumption as well as protect the environment [1]. In the latter, during a severe accident in a nuclear power plant, the exposed molten core from the pressure vessel would interact with the coolant in the ex-vessel [2] and even with the concrete known as Molten Core-Concrete Interaction (MCCI). During MCCI, the molten core consisting of the mixture of oxides and metals [3] forms the horizontal immiscible stratified liquid pool. Because the molten oxide like UO_2 is denser than the molten metal such as steel and sinks, the molten metal floats on the upper layer as shown in Fig. 1. In addition, the denser molten oxide especially UO_2, has high decay power and temperature would heat the concrete. Then the evaporable and chemically bound water and chemically bound CO_2 would be released from concrete forming the gas bubbles. The released gas bubbles rise in the molten pool and stir it to enhance the heat transfer between the liquid layers. In addition, during the process that the bubbles pass though the interface between the denser and lighter liquids, the lower molten oxide would be entrained into the upper molten metal. The heat transfer area between two layers increases significantly, and so does the heat transfer. Werle [4] found that the entrainment at the overlying immiscible layers caused by gas bubbles plays a significant role in the heat transfer while the pure natural convection only plays a minor role. And Suo-Anttila [3] proposed that if the entrainment rate caused by bubbles is obtained, it is easy to predict the heat transfer at interface between overlying layers. In addition, the temperature gradient at the interface decreases because of bubble stirring, which decreases the temperature of the denser liquid and mitigates the MCCI. Therefore, the investigation of the mass transfer at the interface between overlying layers caused by bubbles is of great significance for the

* Corresponding author.
** Corresponding author.
E-mail addresses: rhchen@mail.xjtu.edu.cn (R. Chen), ghsu@mail.xjtu.edu.cn (G.H. Su).

https://doi.org/10.1016/j.net.2019.11.023

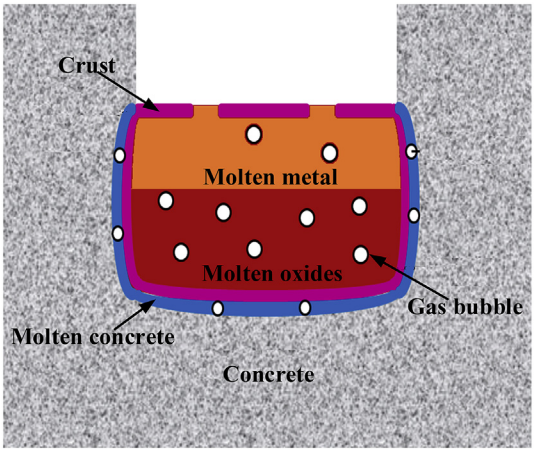

Fig. 1. The sketch of the immiscible layers in MCCI [37].

analysis of the MCCI. And many researchers have studied this phenomenon.

Based on unsteady state, Szekely [5] derived the mathematical model for heat and mass transfer under the influence of successive bubbles. Werle [4] studied the enhancement of heat transfer between overlying layers under the influence of gas flow rate through experiments of oil-water and oil-Wood's metal. The heat transfer coefficient increased significantly in the experiment. Green [6–8] theoretically investigated the entrainment volume by single bubble based on force balance. In his study, if entrainment occurs, the threshold for the density ratio of different liquids is 3. Additionally, the effects of bubble velocity, density, viscosity and interface tension force on entrainment performance were analyzed. The theoretical results agreed well with the experiments of oil-water and oil-Wood's metal. Shaw [9] investigated the behaviors of droplets including the number, the size distribution and the coalescence time of them experimentally as well as theoretically after bubble passes through the interface. But these investigations primarily focused on the entrainment of the denser liquid in bubble wake. Han [10] found that there were two models for the formation of denser droplets. The first is the entrainment at the wake of the bubble as mentioned above. And the second is the rupture of the film on the bubble. Song [11,12] further investigated these two models in Lead-salt system. The ascending/descending velocity of droplet was obtained according to the theory.

The above investigations are all based on the theory or experiment. While in the field of numerical simulation, since the mass transfer characteristics at immiscible liquids interface entrained by a single bubble is a complicated and comprehensive phenomenon with violent interface distortion it is difficult to be simulated, especially the simulation of the film on the bubble. In recent years, numerical simulation methods have been rapidly developed and widely applied in many fields. Except the traditional grid methods, the Lagrangian meshless methods have attracted much more attention for its outstanding advantages in surface tracking. Among these methods, the Moving Particle Semi-implicit (MPS) method proposed by Koshizuka [13] has shown a great capability to capture free surfaces. And in the investigation of the severe accident, many investigations have been carried out using MPS method [14–17]. In the fields of multiphase flow simulation, two categories have been developed [18]. The first one is coupling MPS method with other methods, such as MPS-MAFL [19] and MPLS [20]. The different phases are handled with different methods in this category. Tian [21–23] and Chen [24–26] have developed the MPS-MAFL method and simulated bubble dynamics successfully. The second is that the different phases are all handled as particles and the key point in this category is to solve the discontinuities at the interface. Duan [27] proposed a multiphase MPS method called MMPS. The stability is enhanced significantly. Whereafter, Guo [28] further developed this method which makes it more stable and applicable.

In this study, the developed MMPS method [28] and the improved interface tension force model are adopted to investigate the mass transfer at immiscible liquids interface caused by single bubble rising. The properties of different liquids are all their actual value replacing the artificial properties such as the surface tension force and the viscosity in order to promote the applications of MPS in engineering. Correspondingly, the influences of bubble size, the density ratio between two liquids, and the interface tension force on the mass transfer characteristics are investigated in depth.

1.1. Multiphase moving particle semi-implicit (MMPS) method

In MPS method, the fluid is discretized as particles and the fluid flow is represented by the particles' motion. The governing equations are mass and momentum conservation equations. And the terms in these two equations are discretized as the interaction between particles. In the field of the multiphase flow simulation, the problem with the MPS method is the discontinuity at interface, which could cause the computation instability. In this study, the MPS method for multiphase flow proposed by Duan [27] and the improved schemes proposed by Guo [28] are adopted to simulate the entrainment at the immiscible layers caused by single bubble which is an important phenomenon in MCCI.

1.2. Governing equations

The mass and momentum conservation equations for incompressible fluid are represented as follows:

$$\frac{D\rho}{Dt}+\rho\nabla\cdot\vec{u}=0 \tag{1}$$

$$\frac{D\vec{u}}{Dt}=-\frac{1}{\rho}\nabla p+\frac{1}{\rho}\nabla\cdot(\mu\nabla\vec{u})+\vec{g}+\frac{1}{\rho}\vec{F}_S \tag{2}$$

where ρ, $\vec{u}$, p, μ, $\vec{g}$ and $\vec{F}_S$ are density, velocity, pressure, dynamic viscosity coefficient, gravity and surface tension force respectively. The values of density ρ and dynamic viscosity coefficient μ are constants in each type of particles or fluids, while at interface the values of them change dramatically which would cause numerical instability. In addition, the surface/interface tension force is important for multiphase flow. In MPS method, there are many different calculation schemes for the surface/interface tension force $\vec{F}_S$. In this study, the Contoured Continuum Surface Force (CCSF) method proposed by Duan [29] is adopted to calculate the surface/interface tension force in multiphase flow which is a high precision method.

1.3. Pressure calculation

In MPS method, the pressure is solved by Pressure Poisson Equation (PPE). In this study, the PPE reads as follows [27]:

$$\left\langle\nabla\cdot\left(\frac{1}{\rho}\nabla p\right)\right\rangle_i^{k+1}=\frac{(1-\gamma)}{\Delta t}\nabla\cdot\vec{u}^*-\frac{\gamma}{\Delta t^2}\frac{n^0-n_i^*}{n^0}+\frac{\alpha}{\Delta t^2}P_i^{k+1} \tag{3}$$

where the superscript $k+1$ represents the parameters at next calculation time step, the superscript * represents the temporary parameters, and n^0 is the constant particle number density. The γ

Please cite this article as: C. Dong et al., Simulation on mass transfer at immiscible liquid interface entrained by single bubble using particle method, Nuclear Engineering and Technology, https://doi.org/10.1016/j.net.2019.11.023

and α represent the adjustment coefficient and the coefficient of compressibility. Their values in this study are 0.05 and 10^{-6} respectively.

The right hand side of Eq. (3) is the mixture source term of PPE replacing the standard one [13] which could improve the numerical stability in the simulation of multiphase flow. The left hand side of Eq. (3) is discretized by a higher order Laplacian model [30] replacing the original model [13]. The formation in 2D is shown as follows:

$$\langle \nabla \cdot \left(\frac{1}{\rho} \nabla p \right) \rangle_i^{k+1} = \frac{1}{n_0} \sum_{j \neq i} \left[\frac{2}{\rho_i + \rho_j} \left(P_{ij} \frac{\partial^2 w_{ij}}{\partial r_{ij}^2} - \frac{P_{ij}}{r_{ij}} \frac{\partial w_{ij}}{\partial r_{ij}} \right) \right] \tag{4}$$

The pressure distribution could be calculated through solving above two equations. And the pressure gradient term in momentum conservation equation is calculated according to the pressure distribution. In order to promote the accuracy of the pressure gradient at the interface, it is calculated as follows:

$$\left\langle \frac{1}{\rho} \nabla p \right\rangle_i = \frac{d}{n_0} \sum_{j \neq i} \left\{ \frac{2\left(p_j - p_i\right)\left(\vec{r}_j - \vec{r}_i\right)}{(\rho_i + \rho_j) r_{ij}^2} C_{ij} w_{ij} \right\} + \frac{d}{n_0} \sum_{j \neq i} \left\{ \frac{\left(p_i - p'_{i,\min}\right)\left(\vec{r}_j - \vec{r}_i\right)}{(\rho_i + \rho_j) r_{ij}^2} C_{ij} w_{ij} \right\} \tag{5}$$

where d is the number of dimensions, $p'_{i,\min}$ is the minimum pressure of particle around the target particle i with the same type, and C_{ij} is a dimensionless corrective matrix to improve the accuracy.

1.4. The viscosity term calculation

The discontinuity of viscosity at interface is another problem which could also cause the numerical instability. The artificial viscosity is always adopted in the previous simulations [31], which is effective to prevent the penetration at the interface. In this study, another scheme proposed by Duan [27] is adopted. The harmonic average viscosity coefficient and arithmetic average density are utilized as follows:

$$\langle \frac{1}{\rho} \nabla \cdot (\mu \nabla \vec{u}) \rangle_i = \frac{18d}{r_e^2} \sum_j \frac{2\mu_i \mu_j}{\mu_i + \mu_j} \frac{2}{\rho_i + \rho_j} (\vec{u}_j - \vec{u}_i) G_{ij} \tag{6}$$

In the above equation, the viscosity of target particle i is also taken into consideration. Therefore, the Gaussian function G_{ij} is utilized as the weight function here [21].

1.5. Surface/interface tension force calculation

In the simulation of multiphase flow, there are many ways to compute the surface/interface tension force. The one is the Interparticle Potential (IP) method proposed by Shirkawa [32,33]. It is relatively simpler and could save computing time. But it is an artificial method, and some coefficients are adjusted according to the simulation case. In addition, the calculation accuracy depends on the resolution while the results is difficult to be convergent as the resolution increases. In this study, another method called the Contoured Continuum Surface Force model [29] is utilized. The surface/interface tension force is calculated as follows:

$$\vec{F}_s = \sigma \cdot \kappa \cdot \nabla C \tag{7}$$

where σ is the surface/interface tension coefficient, κ is the interface curvature, and C is the color function which is defined as follows:

$$C_j = \begin{cases} 0 & \text{if j is in the specified type} \\ 1 & \text{if j is in the other type} \end{cases} \tag{8}$$

In this study, the above equation is treated that if the type of particle j is similar with the type of target particle i, the value of the color function is equal to 0. Otherwise, it is equal to 1. And the interface curvature κ is calculated according to the first-order Taylor expansion of the smoothed color function. Due to its complex form, the details could be found in reference [29] and it is omitted in this study. In this study, the bubble would rise in the denser liquid and pass through the interface between the two liquids. The bubble, the denser liquid and the lighter liquid would contact with each other and the surface tension coefficient σ is no longer a constant. Therefore it is calculated as Eqs. (9) and (10) in this study:

On the basis of the "Antonoff's rule", the interface tension coefficient between liquid1 and liquid2 is calculated as follows:

$$\sigma_{12} = |\sigma_1 - \sigma_2| \tag{9}$$

where σ_1 and σ_2 are the surface tension coefficients of liquid1 and liquid2, respectively. Whilst, in order to ensure the continuity at the interface, the interface tension coefficient of target particle i is calculated as follows:

$$\langle \sigma \rangle_i = \frac{\sum_{j \neq i} \sigma_{ij} w_{ij}}{\sum_{j \neq i} C_j w_{ij}} \tag{10}$$

Compared with the method adopted by Natsui [34,35], this method emphasizes the influence of particles near the interface through the weight function. And the continuity of the interface tension coefficient is maintained.

Specifically, the acceleration continuity at the interface induced by the interface tension force is another problem. If the actual density of target particle i is utilized, the acceleration of the lighter particle is obviously greater than that of the denser particles, resulting in interface discontinuity. On the contrary, if the smoothed density is adopted, the penetration at the interface is easy to occur. In this study, the density of target particle i is calculated as follows:

$$\rho_{s,i} = \frac{\rho_i + \langle \rho \rangle_i}{2} \tag{11}$$

where $\rho_{s,i}$ is the density of particle i adopted in the interface tension force term. ρ_i is the actual density of particle i, and $\langle \rho \rangle_i$ is the smoothed density of particle i [28].

Taking Eqs. (10) and (11) into the momentum conservation equation, the interface tension force in the momentum conservation equation could be rewritten as follows:

$$\langle \frac{1}{\rho} \vec{F}_s \rangle = \frac{\langle \sigma \rangle_i \cdot \kappa \cdot \nabla C}{\rho_{s,i}} \tag{12}$$

2. Validation of the code

2.1. Validation of surface/interface tension model

In order to validate the surface/interface tension model adopted in this study, the case that a square droplet deforms only under the influence of interface tension force is tested. The parameters of liquids are shown in Table 1. So as to eliminate the influence of

Please cite this article as: C. Dong et al., Simulation on mass transfer at immiscible liquid interface entrained by single bubble using particle method, Nuclear Engineering and Technology, https://doi.org/10.1016/j.net.2019.11.023

Table 1
Parameters in the validation of surface/interface tension model.

Fluid	Density/kg·m^{-3}	Dynamic viscosity/N·s·m^{-2}	Surface tension coefficient N·m^{-1}
Liquid1	1000	1.002×10^{-3}	0
Liquid2	1000	1.002×10^{-3}	5.0475×10^{-2}

gravity, the densities of the liquid1 and liquid2 are similar. The initial geometry of the test case is shown in Fig. 2 (a). The square droplet of liquid1 deforms at different times as shown in Fig.2 (b)–(g). Because of the viscosity, the oscillation amplitude gradually decreases. And at about 0.68s, the shape of the droplet would remain stable. In addition, the effect that the surface/interface tension force maintains the interface smooth and prevents the penetration would be expressed in the Section 3.2.

2.2. Validation by the droplet rising

The case of droplet rising is always utilized to test the capability of the multiphase simulation [30]. There is a benchmark adopted to validate the code. In order to bring into correspondence with the benchmark, the scale and the parameters are all converted into proper dimensionless indexes. The calculation domain of the test case and the initial particle arrangement are shown in Fig. 3. The droplet of liquid1 is spherical and static initially. Then it rises and deforms in the liquid2. The boundaries are all no slip walls. The parameters of the liquids are listed in Table .2. At different times, the shape of the droplet and the pressure distribution are shown in Fig. 4. The Eo ($Eo = g\Delta\rho d_e^2/\sigma$) is a criterion to judge the breakup of the droplet in experiment. When the droplet breakup occurs in this study, the value of Eo is larger than the threshold value 16 owing to the surface/interface tension force adopted in this study. In order to prove that the surface/interface tension model adopted in this study has the good capability to maintain the interface smooth and prevent the penetration. The particle distributions at the droplet top (as shown inside the boxes of Fig. 4) at different times are shown in Fig. 5. There is a distinct interface between two liquids. In addition, the calculated rise velocity using MPS method is shown in Fig. 6 compared with the result of TP2D [36]. Through the comparison, the trend of the calculated velocity using MPS method is similar with the benchmark but it is slower in MPS method. There are two main reasons causing this result: Firstly, the acceleration caused by surface/interface tension force is not continuous which is like that there is an extra force at the interface. The efficient of this surface/interface tension model is obvious. But it also introduces a certain error into the calculation. Secondly, the viscosity model adopted in this study lacks of accuracy [28]. There is still some work to be done to improve its accuracy.

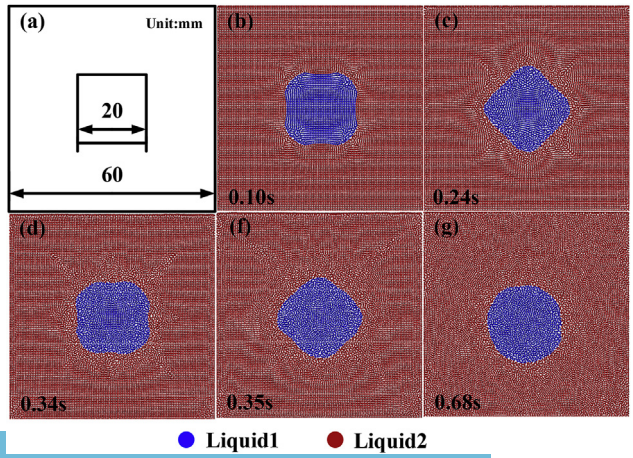

Fig. 2. The deformation of the square droplet over time.

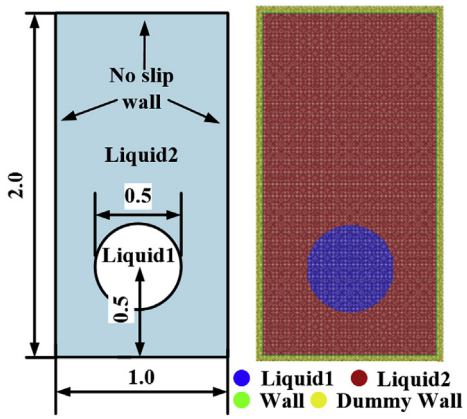

Fig. 3. The calculation domain and the initial particle arrangement in the validation by the droplet rising.

Table 2
Parameters of droplet rising.

Fluid	Density	Dynamic viscosity	Surface tension coefficient	Gravity
Liquid1	1	0.1	1.96	0.98
Liquid2	1000	10		

2.3. Validation by comparison with experimental results

Natsui [34] carried out an experiment in which the gas bubble stirred the water-oil interface. The geometry of the experiment in 2D and the initial particle arrangement in calculation are shown in Fig. 7. Since the uppermost layer of the experiment is gas, it is treated as a free surface in calculation which could decrease the calculation time. In addition, the physical properties could be found in reference [34]. In this case, the density ratio of the two liquids is close to 1, therefore the entrainment is quite violent, forming a complex oil-water interface. Fig. 8 shows the comparison on the height of the entrained water over time between the experiment and the calculation result. The trend is similar especially after the film ruptures. But the calculated entrained water height is lower than the experimental value simultaneously. Firstly, the calculation error causes this result as mentioned in section 3.2. Secondly, the initial state of the bubble in the calculation is static, while in the experiment, the bubble is released from the plastic cup. When the plastic cup and the nichrome rod roll, the water around the bubble would be stirred. And the bubble would get an acceleration. In addition, the initial shape of the bubble is completely spherical in the simulation. The bubble deforms firstly and it almost keeps static in position. While in the experiment, the bubble is controlled by the hemispheric cup, and it has deformed before it is released. When it is released, the time of bubble deformation is less than that in the simulation. Thirdly, errors are inevitable due to the use of 2D

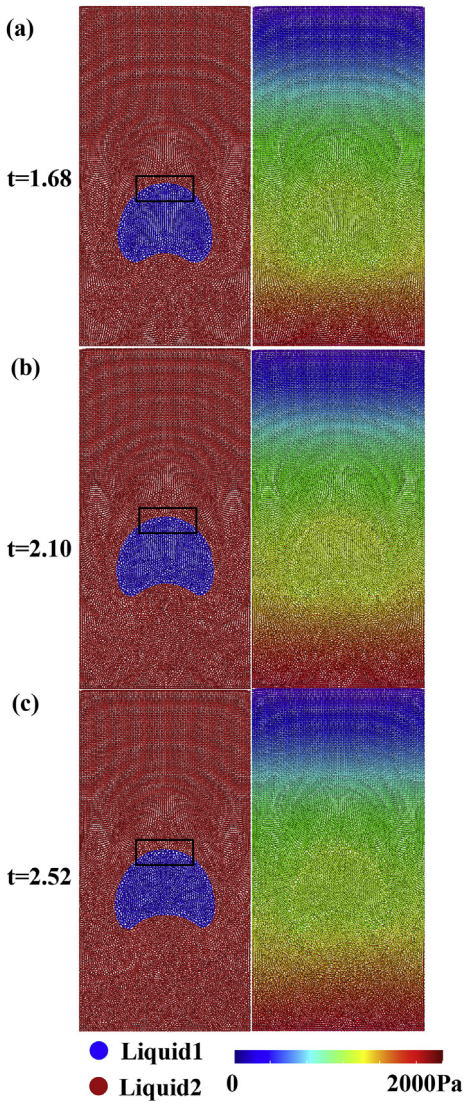

Fig. 4. The shape of the droplet and the pressure distribution at different times.

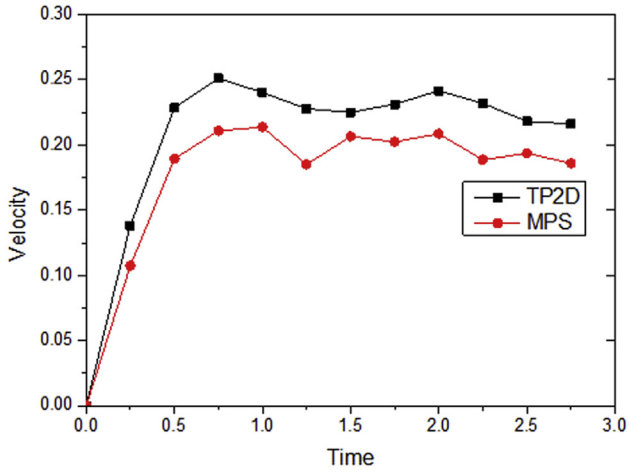

Fig. 6. Comparison of droplet velocity between the calculated results of MPS and TP2D.

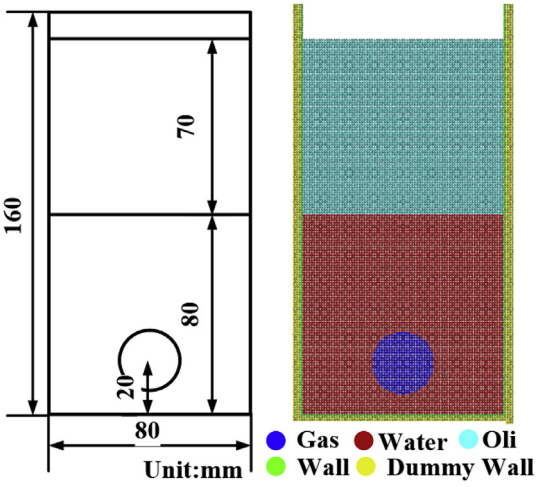

Fig. 7. The sketch of experiment geometry in 2D and the initial particle arrangement in MPS.

numerical simulation. And compared with the images when the bubble locates at the same height as shown in Fig. 9, the disorder interface of the entrained column is successfully simulated. In Fig. 9 (a), the very thin water film on the bubble is well simulated. In Fig. 9 (b), the bubble rises in the oil, and the entrained water column is formed under the bubble. But because this case is simulated in 2D and the fluid flow in radial direction is neglected, the water falls even lower than that in experiment. In Fig. 9 (c), the bubble rises to the free surface. At the root of the column, two parts are formed: a thin column in the middle and a bilaterally expanded part which is similar to the experiment. The middle thin column is formed because of the shrink of the column. The bilateral expanded part is formed because the density ratio between two liquids is near 1. When the denser liquid falls, it could expand in the horizontal direction like R-T (Rayleigh-Taylor) instability. But if the density difference is large enough, this phenomenon is difficult to happen.

3. Results and discussion

In this section, the mass transfer characteristics at immiscible liquid interface stirred by single bubble will be analyzed and summarized. Besides, the influence of bubble size, density ratio between two liquids and interface tension force on the height of the entrained column over time will be introduced and discussed in this section.

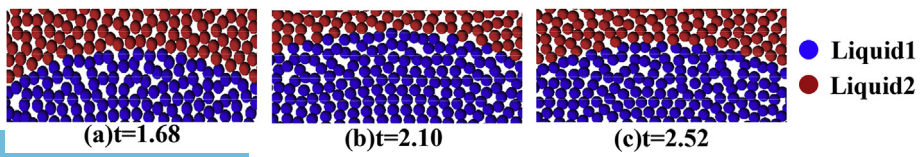

Fig. 5. The smooth interface of the bubble top at different times.

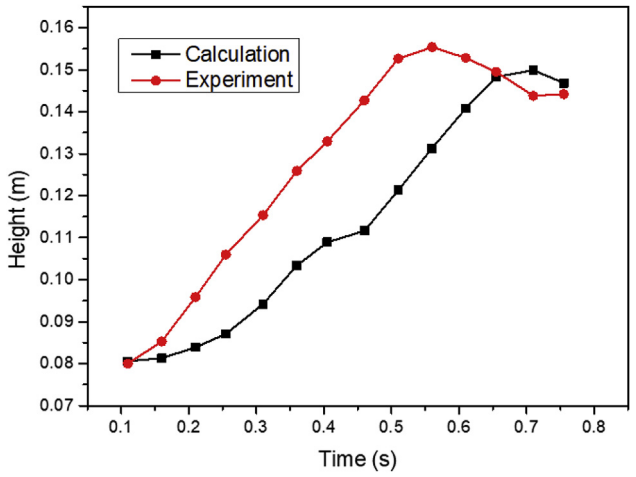

Fig. 8. Comparison on the height of the entrained water over time between the experiment and calculation.

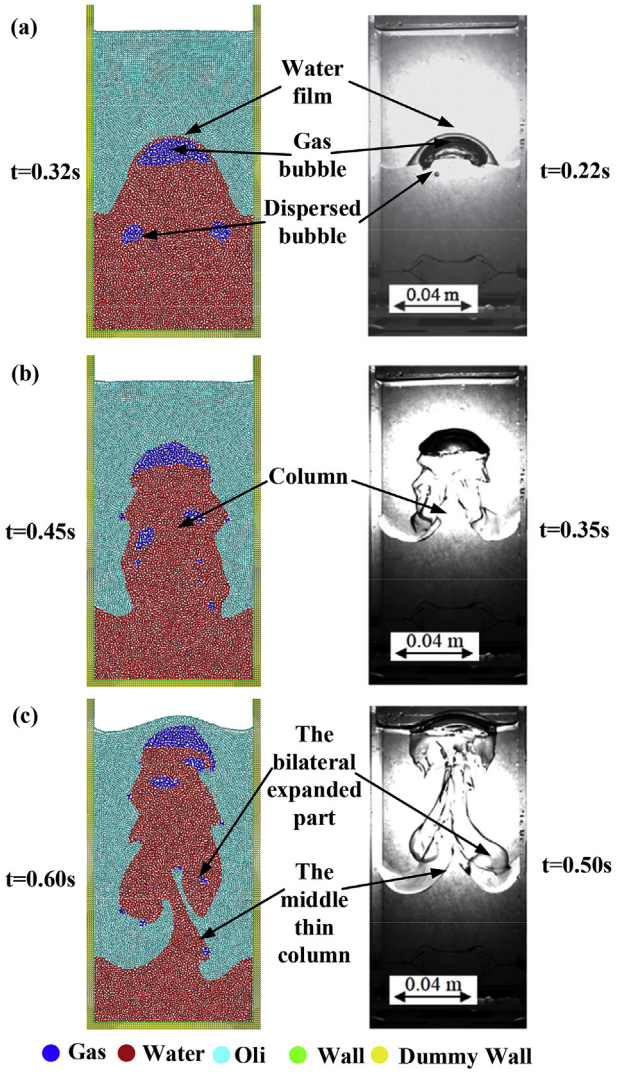

Fig. 9. Comparison of the images between the simulation results and the experiment results.

3.1. The influence of bubble size

When MCCI occurs, the decay heat decreases with time and the efficiency of the melt core-concrete interaction would vary. The efficiency of released gas would also change, which could influence the bubble size and the entrainment at the immiscible liquid interface. In this section, the influence of bubble size on the characteristics of mass transfer would be investigated. The calculation domain is shown in Fig. 10. In order to decrease the influence of the boundary, the weight of the calculation domain is 120 mm, which is more than 4 times the diameter of the bubble. The bubble diameters are 24 mm, 20 mm and 18 mm respectively. The other parameters are shown in Table .3. The density ratio between the two liquids is 2 in this section, because in the study of Green [6], he found that entrainment is difficult to occur if the density ratio exceeds 3. Fig. 11 shows the change of the height of the entrained denser liquid over time. From the figure, we can find that the height of the entrained denser liquid is higher with the increase of the bubble size simultaneously. In addition, since the larger the bubble is, the flatter the top becomes, and more denser liquid on the top of the bubble when it passes through the interface. The time of film rupture above the bubble is similar. While the velocity is larger with the increase of the bubble size when it passes through the interface. Although the bubble height is quite different, the time of the film breakup is close to each other.

3.2. The influence of density ratio between two liquids

The density ratio between two liquids is an important parameter influencing the mass transfer at immiscible liquid interface. In MCCI, because the molten concrete would rise up into molten core, the density ratio between different layers would change. In this section, the density ratio between two liquids is investigated. The calculation domain is similar with Fig. 10. The parameters are shown in Table .4. The density of the denser liquid is 1000 kg m^{-3}, and the density ratio is varied by changing the density of the lighter liquid. The calculation results of the height of the entrained denser liquid over time is shown in Fig. 12. Before the denser liquid film ruptures, the height of the entrained denser liquids does not differ much, because in these cases, the denser liquids have the same density, and the bubble rising velocity is same with each other. While after the film ruptures, the difference gradually occurs. The smaller the density ratio is, the higher the entrained denser liquid is. And when the density ratio is large enough, the entrained column falls rapidly and a significant concave surface is formed.

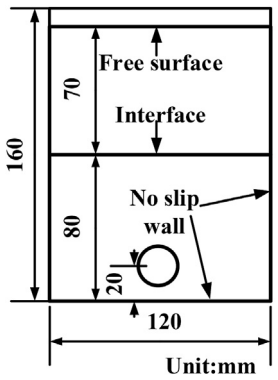

Fig. 10. The calculation domain in section 4.

Table 3
Parameters in the influence of bubble size.

Fluid	Density/kg·m^{-3}	Dynamic viscosity/N·s·m^{-2}	Surface tension coefficient/N·m^{-1}
Lighter liquid	500	0.01	2.09×10^{-2}
Denser liquid	1000	0.001	7.20×10^{-2}
Gas	1.18	0.0001	0

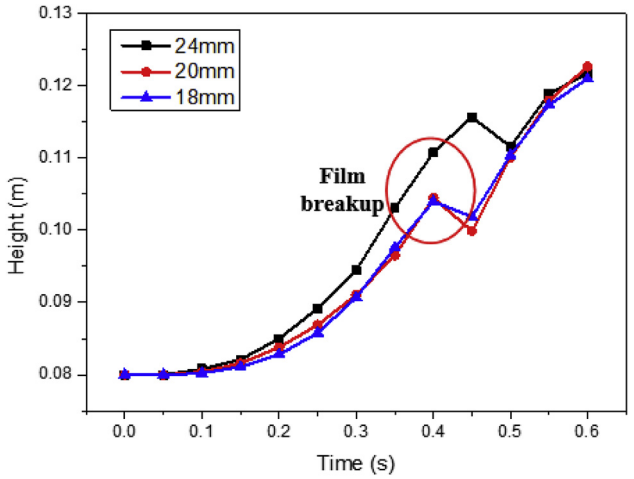

Fig. 11. The height of the entrained denser liquid over time with different bubble sizes.

Table 4
Parameters in the influence of density ratio.

Fluid	Density/kg·m^{-3}	Dynamic viscosity/N·s·m^{-2}	Surface tension coefficient/N·m^{-1}	Bubble size/mm
Lighter liquid	–	0.01	2.09×10^{-2}	20
Denser liquid	1000	0.001	7.20×10^{-2}	
Gas	1.18	0.0001	0	

3.3. The influence of interface tension force

The interface tension force is another factor that could influence the mass transfer characteristics stirred by bubbles in MCCI. In the theory of Green [6], the interface tension force on the bubble is supposed to have a maximum contact angle before the bubble passing through the interface. The results based on this theory may be too conservative because the interface tension force is larger than that in the actual situation. In this section, the influence of interface tension force on mass transfer characteristics at immiscible liquid interface is investigated. The calculation domain is similar with Fig. 10, too. And the parameters in the simulation are listed in Table .5. In order to change the interface tension force, the surface tension coefficient of denser liquid is changed.$7.20 \times 10^{-2} N \cdot m$,$12.31 \times 10^{-2} N \cdot m$ and$22.53 \times 10^{-2} N \cdot m$ are adopted as the surface tension coefficient of denser liquid in different cases. And the interface tension coefficients between two liquids are$5.11 \times 10^{-2} N \cdot m$,$10.22 \times 10^{-2} N \cdot mand20.44 \times 10^{-2} N \cdot m$respectively. Fig. 13 shows the change of height of the entrained column over time under different interface tension coefficients. Before the denser liquid film ruptures, the height of the denser liquid over time is similar under different cases. But after the film ruptures, the denser liquid falls rapidly under the larger interface tension coefficient because of the larger interface tension force is like an extra force.

Table 5
Parameters in the influence of interface tension force.

Fluid	Density/kg·m^{-3}	Dynamic viscosity/N·s·m^{-2}	Surface tension coefficient/N·m^{-1}	Bubble size/mm
Lighter liquid	500	0.01	2.09×10^{-2}	20
Denser liquid	1000	0.001	–	
Gas	1.18	0.0001	0	

4. Conclusions

In this study, the improved MMPS has been utilized to simulate the mass transfer characteristics at immiscible liquids interface stirred by single bubble which is an important phenomenon in MCCI. The influence of bubble size, the density ratio between different liquids, and the interface tension force on the mass transfer characteristics are investigated in this study. The simulation results have shown as follows:

1) The bubble size has certain influence on the characteristics of the height of the entrained denser liquid. With the increase of the bubble size, the height of the entrained denser liquid is

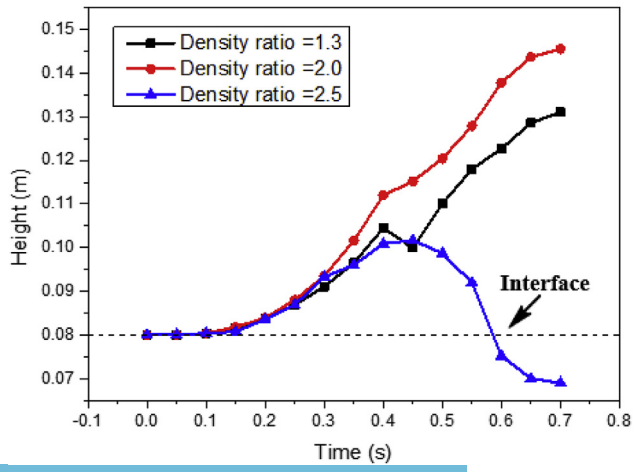

Fig. 12. The height of the entrained denser liquid over time with different density ratios.

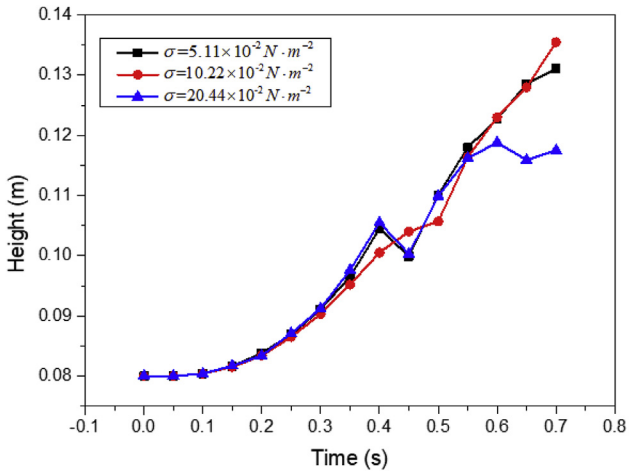

Fig. 13. The height of the entrained denser liquid over time with different interface tension coefficients.

higher at the same time. Because the larger bubble has the larger velocity.

2) The influence of the density ratio between two liquids on the mass transfer characteristics is significant. When the density ratio is 2.5 (close to 3, the density ratio threshold of entrainment presented by Green [6]), the entrained denser liquid falls rapidly and the height of the entrained denser liquid is significantly lower than other cases. This phenomenon is mainly caused by the decrease of buoyancy on the entrained denser liquid.
3) With the increase of the interface tension force, the column falls more rapidly because the increasing interface tension force applies an opposite extra force on the entrained denser liquid.

Acknowledgments

The present study is supported by the National Science Foundation of China (No. 11875217, 11505134), the National Natural Science Foundation of China outstanding youth fund (11622541) and the Young Elite Scientists Sponsorship Program by CAST (2018QNRC001).

Appendix A. Supplementary data

Supplementary data to this article can be found online at https://doi.org/10.1016/j.net.2019.11.023.

References

[1] D.Y. Song, N. Maruoka, T. Maeyama, et al., Influence of bottom bubbling condition on metal emulsion formation in lead-salt system, ISIJ Int. 50 (11) (2010) 1539–1545.
[2] R.H. Chen, J. Wang, G.H. Su, et al., Analysis of KROTOS KS-2 and KS-4 steam explosion experiments with Texas-VI, Nucl. Eng. Des. 309 (1) (2016) 104–112.
[3] A.J. Suo-Anttila, The Mixing of Immiscible Liquid Layers by Gas Bubbling. Division of Reactor System Safety, Office of Nuclear Regulatory Research, U.S, Nuclear Regulatory Commission, 1988.
[4] H. Werle, Enhancement of heat transfer between two horizontal liquid layers by gas injection at the bottom, Nucl. Technol. 59 (1) (1982) 160–164.
[5] J. Szekely, Mathematical model for heat or mass transfer at the bubble-stirred interface of two immiscible liquids, Int. J. Heat Mass Transf. 6 (5) (1963) 417–422.
[6] G.A. Green, J.C. Chen, M.T. Conlin, Onset of entrainment between immiscible liquid layers due to rising gas bubbles, Int. J. Heat Mass Transf. 31 (6) (1988) 1309–1317.
[7] G.A. Green, J.C. Chen, T.F. Irvien, Heat transfer between stratified immiscible liquid layers driven by gas bubbling across the interface, in: ANS Proceedings of the National Heat Transfer Conference, Houston, TX, 1988.
[8] G.A. Green, J.C. Chen, M.T. Conlin, Bubbling induced entrainment between stratified liquid layers, Int. J. Heat Mass Transf. 34 (1) (1991) 149–157.
[9] J.M. Shaw, R. Konduru, The behaviour of large gas bubbles at a liquid-liquid interface. Part 2: liquid entrainment, Can. J. Chem. Eng. 70 (1992) 381–384.
[10] Z.J. Han, L. Holappa, Mechanisms of iron entrainment into slag due to rising gas bubbles, ISIJ Int. 43 (3) (2003) 292–297.
[11] D.Y. Song, N. Maruoka, T. Maeyama, H. Shibata, et al., Influence of bottom bubbling condition on metal emulsion formation in lead-salt system, ISIJ Int. 50 (11) (2010) 1539–1545.
[12] D.Y. Song, N. Maruoka, G.S. Gupta, et al., Modeling of ascending/descending velocity of metal droplet emulsified in Pb-salt system, Metall. Mater. Trans. B 43 (4) (2012) 973–983.
[13] S. Koshizuka, Y. Oka, Moving-particle semi-implicit method for fragmentation of incompressible fluid, Nucl. Sci. Eng. 123 (3) (1996) 421–434.
[14] R.H. Chen, Q.H. Cai, P.H. Zhang, et al., Three-dimensional numerical simulation of the HECLA-4 transient MCCI experiment by improved MPS method, Nucl. Eng. Des. 347 (2019) 95–107.
[15] R.H. Chen, K.L. Guo, Y.S. Zhang, et al., Numerical analysis of the granular flow and heat transfer in the ADS granular spallation target, Nucl. Eng. Des. 330 (2018) 59–71.
[16] R.H. Chen, Y.L. Li, K.L. Guo, et al., Numerical investigation on the dissolution kinetics of ZrO2 by molten zircaloy using MPS method, Nucl. Eng. Des. 319 (2017) 117–125.
[17] R.H. Chen, L. Chen, K.L. Guo, et al., Numerical analysis of the melt behavior in a fuel support piece of the BWR by MPS, Ann. Nucl. Energy 102 (2017) 422–439.
[18] R.H. Chen, C.H. Dong, K.L. Guo, et al., Current achievements on bubble dynamics analysis using MPS method, Prog. Nucl. Energy 118 (2020) 1–11.
[19] H.Y. Yoon, S. Koshizuka, Y. Oka, A mesh-free numerical method for direct simulation of gas-liquid phase interface, Nucl. Sci. Eng. 133 (2) (1999) 192–200.
[20] J. Liu, S. Koshizuka, Y. Oka, A hybrid particle-mesh method for viscous, incompressible, multiphase flows, J. Comput. Phys. 202 (1) (2005) 65–93.
[21] W.X. Tian, Y. Ishiwatari, S. Ikejiri, et al., Numerical simulation on void bubble dynamics using moving particle semi-implicit method, Nucl. Eng. Des. 239 (11) (2009) 2382–2390.
[22] W.X. Tian, Y. Ishiwatari, S. Ikejiri, et al., Numerical computation of thermally controlled steam bubble condensation using Moving Particle Semi-implicit (MPS) method, Ann. Nucl. Energy 37 (1) (2010) 5–15.
[23] W.X. Tian, R.H. Chen, J.L. Zuo, et al., Numerical simulation on collapse of vapor bubble using particle method, Heat Transf. Eng. 35 (6–8) (2014) 753–763.
[24] R.H. Chen, W.X. Tian, G.H. Su, et al., Numerical investigation on bubble dynamics during flow boiling using moving particle semi-implicit method, Nucl. Eng. Des. 240 (11) (2010) 3830–3840.
[25] R.H. Chen, W.X. Tian, G.H. Su, et al., Numerical investigation on coalescence of bubble pairs rising in a stagnant liquid, Chem. Eng. Sci. 66 (21) (2011) 5055–5063.
[26] R.H. Chen, M.H. Zhang, K.L. Guo, et al., Numerical study of bubble rising and coalescence characteristics under flow pulsation based on particle method, Science and Technology of Nuclear Installations (2019) 2045751.
[27] G.T. Duan, B. Chen, S. Koshizuka, et al., Stable multiphase moving particle semi-implicit method for incompressible interfacial flow, Comput. Methods Appl. Mech. Eng. 318 (2017) 636–666.
[28] K.L. Guo, R.H. Chen, S.Z. Qiu, et al., An improved multiphase moving particle semi-implicit method in bubble rising simulations with large density ratios, Nucl. Eng. Des. 340 (2018) 370–387.
[29] G.T. Duan, S. Koshizuka, B. Chen, A contoured continuum surface force model for particle methods, J. Comput. Phys. 298 (2015) 280–304.
[30] A. Khayyer, H. Gotoh, A higher order Laplacian model for enhancement and stabilization of pressure calculation by the MPS method, Appl. Ocean Res. 32 (1) (2010) 124–131.
[31] S. Natsui, H. Takai, T. Kumagai, et al., Stable mesh-free moving particle semi-implicit method for direct analysis of gas-liquid two-phase flow, Chem. Eng. Sci. 111 (2014) 286–298.
[32] N. Shirakawa, H. Horie, Y. Yamamoto, et al., Analysis of the void distribution in a circular tube with the two-fluid particle interaction method, J. Nucl. Sci. Technol. 38 (6) (2001) 392–402.
[33] N. Shirakawa, Y. Yamamoto, H. Horie, et al., Analysis of subcooled boiling with the two-fluid particle interaction method, J. Nucl. Sci. Technol. 40 (3) (2003) 125–135.
[34] S. Natsui, H. Takai, T. Kumagai, et al., Multiphase particle simulation of gas bubble passing through liquid/liquid interfaces, Mater. Trans. 55 (11) (2014) 1707–1715.
[35] S. Natsui, R. Nashimoto, H. Takai, et al., SPH simulations of the behavior of the interface between two immiscible liquid stirred by the movement of a gas bubble, Chem. Eng. Sci. 141 (2016) 342–355.
[36] S. Hysing, S. Turek, D. Kuzmin, et al., Quantitative benchmark computations of two-dimensional bubble dynamics, Int. J. Numer. Methods Fluids 60 (11) (2009) 1259–1288.
[37] X. Li, A. Yamaji, A numerical study of isotropic and anisotropic ablation in MCCI by MPS method, Prog. Nucl. Energy 90 (2016) 46–57.